KfK 5217
September 1993

Report on HFR Power Cycling Experiment MEDINA/POCY 02

O. Goetzmann
Institut für Materialforschung
Projekt Nukleare Sicherheitsforschung

Kernforschungszentrum Karlsruhe

Kernforschungszentrum Karlsruhe

Institut für Materialforschung

Projekt Nukleare Sicherheitsforschung

KfK 5217

Report on HFR Power Cycling Experiment MEDINA/POCY 02

O. Goetzmann

Kernforschungszentrum Karlsruhe GmbH, Karlsruhe

Als Manuskript gedruckt

Kernforschungszentrum Karlsruhe GmbH
Postfach 3640, 76021 Karlsruhe

ISSN 0303-4003

Abstract

MEDINA or POCY 02 was a single pin experiment to study power ramp induced FCMI with the smear density as parameter. Four separate fuel columns with different void volume redistribution were intergrated in one pin. The irradiation device should allow for the measurement of the pin diameter along all fuel columns after each power cycle. Irradiation took place in the Pool Side Facility of the HFR in Petten from October 1985 through January 1988. The experiment had to be terminated prematurely due to mishandling of the capsule.

The in-pile diameter measurements were of no use. Even though the primary goal was not attained, the experiment furnished some interesting insights into the fuel behaviour during cyclic operation. Mechanical interactions between fuel and cladding took place in all four fuel columns. Maximum pin diameter increase observed was 0,2 %. The largest value was measured in the pin section where the original gap was the largest. Apparently, in cyclic operation a large gap does not ease the FCMI situation. Fuel and fission product movements seem to be enhanced by cyclic operation. Large quantities of solid fission products in the central channel and large reaction zones in the gap between fuel and cladding were observed for these short fuel stacks. Both ends of the annular pellet column were closed by fuel condensation. Pore migration was activated throughout the experiment. It was even capable of transporting cladding reaction products into the central hole.

Bericht über das HFR Betriebstransienten-Experiment MEDINA/POCY 02

Zusammenfassung

MEDINA oder POCY 02 war ein Einzelstabexperiment zur Untersuchung mechanischer Wechselwirkungen aufgrund von Leistungsrampen mit der Fülldichte als Parameter. Vier voneinander getrennte Brennstoffsäulen mit unterschiedlicher Leervolumenverteilung waren in einem Stab integriert. Die Bestrahlungskapsel sollte die Messung des Stabdurchmessers über alle Brennstoffsäulen nach jedem Leistungszyklus erlauben. Die Bestrahlung wurde in der Pool Side Facility des HFR Petten in der Zeit vom Oktober 1985 bis Januar 1988 durchgeführt. Wegen eines Handhabungsschadens an der Kapsel mußte es vorzeitig beendet werden.

Die in-pile gemessenen Durchmesserwerte erwiesen sich als nicht brauchbar. Obwohl es mit diesem Versuchsziel nicht geklappt hat, gab es von diesem Experiment einige interessante Einsichten zum Brennstoffverhalten bei zyklischem Betrieb. Mechanische Wechselwirkungen zwischen Brennstoff und Hülle fanden bei allen 4 Brennstoffsäulen statt. Sie führten zu einer Durchmesservergrößerung der Hülle von maximal 0,2 %. Der größte Wert wurde im Stabsabschnitt mit dem größten Brennstoff-Hülle-Spalt gemessen. Im Zyklierbetrieb wird also durch einen großen Spalt die FCMI Situation nicht entspannt.

Brennstoff- und Spaltproduktttransport wird durch den zyklischen Betrieb erhöht. Große Ansammlungen von festen Spaltprodukten im Zentralkanal sowie große Reaktionszonen zwischen Brennstoff und Hülle wurden bei diesen kurzen Brennstoffsäulen gefunden. Beide Enden der Ringtablettensäule waren durch Brennstoffkondensat geschlossen. Porenwanderung blieb bis zum Ende des Experimentes erhalten. Sie war in der Lage, Hüllreaktionsprodukte bis in den Zentralkanal zu transportieren.

Introduction

For HFR/Petten this experiment was the second Power-Cycling experiment and was therefore named POCY-02. At KfK it was concieved to study fuel-clad mechanical interactions (FCMI) as a consequence of power changes. The irradiation device should allow for diameter measurements during the experiment. This special device was developped by JRC Petten and given free of charge to KfK to find out wether such a measuring system was suitable for in-reactor pin diameter recording. The name of this device MEDINA (Measurement of diameter in-pile axial) was adopted for the experiment by KfK. Hence, in all reports from Petten this experiment is referred to as D170 POCY-02 whereas at KfK it is known and referred to as the MEDINA experiment. It was part of the operating transient irradiations programme sponsored by the Project of Fast Breeder Development (PSB), now Project Nuclear Safety Research (PSF) at KfK.

The goal of this irradiation experiment was twofold: first, it should allow to study the effects of fuel-clad mechanical interactions in a non-steady state operation mode as function of burn-up with the fuel smear density as parameter, and, secondly, to be an accompanying experiment to the POUSSIX experiment, irradiated in PHENIX to study FCMI under steady state conditions, where the same four types of fuel were used as in MEDINA. Indeed, to arrange the fuel stacks in MEDINA, pellets of the same fabrication lots as in POUSSIX where used. The only difference being that in MEDINA the various types of fuel were integrated in one single pin.

The design of the fuel pin can be seen in Fig. 1. It had a can of 1.4970 type stainless steel of 7,6 mm outer diameter and a wall thickness of 0,5 mm. Its overall length was 560 mm. Four types of pellets, all (U, Pu)O_2 with natural uranium and between 21 and 22 % plutonium, were used and arranged in separate fuel columns. These four fuel columns, each containing 8 fuel pellets, were interspaced by a stack of two rhodium pellets (each 3 mm thick) and a breeder pellet (~7,5 mm in length, 6,5 mm diameter) in the arrangement Rh-UO_2-Rh. More details about the fuel pellets and their distribution in the pin are given in table 1. This table also lists pin power, fuel and cladding temperatures, and burn-up for each column. The power values are given for full power operation and refer to positions at column ends or the average over the column length, respectively. During intermediate level operation, all these values were about 30 % lower.

Table 1: Fuel, Fuel Pin and Operational Data

Fuel type	I (AUPUC)	II (OKOM)	III (OKOM)	IV (OKOM)
Position (mm) (rel. to C_L)	110,5 to 49	35,5 to - 19,1	- 42,8 to - 105,0	- 118,6 to - 183,5
Pellet outer diam (mm)	6,415	6,325	6,417	6,479
" inner diam (mm)	-	-	1,233	-
Pellet density (g/cc)	10,615	10,445	10,53	10,422
" " (% th. d.)	96,8	95,2	96,0	95,0
Smear density (% th. d.)	91,4	87,4	87,4	91,6
Fuel/clad gap (µm)	185	275	183	121
Column length (mm)	61,5	64,5	62,2	64,9
Fuel mass (g)	21,1	21,2	20,4	22,3
O/M ratio	1,954	1,955	1,957	1,958
Pu/U + Pu	21,9	21,2	21,2	21,2
Pu_f/Pu	71,02	75,78	75,78	75,86
Local form factor min.	0,75	0,99	0.98	0,86
" mean	0,845	0,965	0,99	0,92
" max.	0,75	0,93	1,00	0,97
Loc. burn-up (%) min.	6,05	7,84	8,27	6,92
" (%) mean	6,81	8,13	8,35	7,41
" (%) max.	7,26	8,34	8,44	7,81
Loc. lin. power (W/cm) min.	383	466	495	440
" mean	431	483	500	471
" max.	460	496	505	496
Temperatures:				
max. inner fuel temp (°C)	2495	2741	2576	2479
max. mid-clad temp (°C)	544	562	555	555

Pin length (mm)	560
outer diam (mm)	7,6 ± 0,03
inner diam. (mm)	6,6 ± 0,03
wall thickn. (mm)	0,5
cladding type	steel 1.4970 15 % cw, a

The fuel pin was immersed in stagnant NaK, whilst the experiment was cooled by the reactor water coolant facilities of the PSF. A He/Ne gas mixture between the primary and secondary containments of the carrier, enabled the control of the clad temperature.

The fuel pin profile was measured by means of a fixed and movable anvil, which transmitted a mechanical signal to 2 transducers, which in turn transmitted the signals via a convertor to a chart recorder and a computer for recording discs. The results indicated the axial profile of the pin. To determine the absolute changes and the rotational position, the pin had been equipped with stepped calibration rings and a helical groove.

The temperature along the fuel pin was measured at 6 axial positions in the fuel region with two thermocouples (type K) at each position. The inlet and outlet temperature of the coolant water were taken by three thermocouples at each position. The average of the 3 inlet and outlet readings gave the coolant temperature increase (ΔT).

The irradiation took place in the pool side facility (PSF) of the HFR in Petten from October 1985 till January 1988 and comprised 24 experimental cycles. It had to be terminated after the carrier was damaged due to mishandling. The design of the carrier and the capsule are described in ref. /1/ and also in the performance reports from CEC Petten.

The originally requested irradiation programme, in terms of linear fissile power, is shown in Fig. 2. The idea of having long periods (21 days) at full power (510 W/cm) and short periods (4, 5 days) at low power (360 W/cm) instead of vice versa, was to achieve in a relatively short time (i.e., 7 reactor cycles) a burn-up of 3 at %. At this level it was assumed to get fuel-clad contact, a prerequisite for FCMI. After the initial 7 cycles it was to be decided wether to go on with the same mode of operation for an additional 7 cycles or to change to a mode that was more adequate to induce FCMI, viz, longer periods at an intermediate power followed by ramps to full power. As it turned out, a burn-up of 3 at % was not achieved after 7 cycles. The actual irradiation programme is given in Fig. 3. Also the fact that no clear indication for the onset of FCMI was visible from the inpile diameter measurements, led to the decision to go on with the same type of cycling.

Results

In pile diameter measurements

Diameter measurements were taken after each cycle. The experiment contained facilities to vertically withdraw the fuel pin and rotate it through 14 steps of 22,5° (315° total). At each rotational position an axial profile could be taken. There was no need to take measurements at all positions. The sensor measures the diametral change, hence measurements have been taken only at rotational positions 0, 45°, 90°, 135° and, as a cross check, at 180°. These positions were numbered as rotational position 0, 2, 4, 6 and 8. The values were tabulated for each cycle and each rotational position for axial steps of approx. 10 mm over the entire pin length. From these numbers the changes for every axial position were evaluated after each cycle. The maximal values for the four fuel column sections are recorded in the diagram shown in Fig. 4. It becomes easily clear from this diagram that something went wrong. There is a repeated up and down of the diameter measurements, a behavior which is physically not explainable. A search was undertaken to find the causes or perhaps explanations for this behavior. After the 16th cycle, there was a prolonged reactor stop of about 4 weeks. To check on any thermal influence on the results, measurements were taken at the beginning, in the middle, and at the end of this period. No indication about any influence of the pin or coolant temperature was obtained. Starting with the 18th cycle, the temperature regime was altered. Before, the temperature of the cladding was raised in parallel with the power increase. Such an operation, however, takes off much of the impact of differential thermal expansion of fuel and cladding during power increases. The cladding temperature was to remain constant during all power changes. From the 18th cycle onward this was attempted by changing the composition of the He/Ne gas mixture between the primary and secondary containment in advance of the power increase. Consequently, before a power ramp the temperature was lowered and then raised again to the old level during the power increase.

Out-pile investigation

The experiment ended January 4, 1988. Gamma spectrometry measurements were made eight months later on August 30, 1988; the diametral measurements one year later on Feb. 31, 1989. The circumferential trace line of the diameter measurements for the axial section covering the four fuel columns is shown in Fig. 5. There was a diameter increase over all four fuel columns, but no cladding expansion in the breeder sections between the fuel columns. The maximum

increase appeared over fuel column II with a value of about 15 µm, which corresponds to 0,2 %. The fuel in this region had a smear density of 88 %; the diametral gap between fuel and cladding was here the largest with 275 µm. The fuel column next to this one (column III) with the same smear density of 88 %, made up, however, by annular pellets with a fuel/cladding gap of 183 µm diametral, experienced with 12 - 13 µm (≃ 0,16 %) somewhat less expansion. The two fuel columns with a smear density of 92 % showed very different diameter increases. Column IV, made up of OKOM fuel and a diametral gap of 121 µm, exhibited a cladding expansion of about 14 µm which was only marginally less than the expansion measured for column II. Column I with AUPUC-fuel and a diametral gap of 185 µm, however, showed an expansion of only 7 to 8 µm (=0,1%).

The differences in the diameter increases can best be explained by differences in gap size in combination with pin power and cyclic operation. Smear density alone is an insufficient parameter: The pin power of the two inner fuel stacks was nearly the same. The maximum power position and the highest average pin power over the fuel stack was in column III, though. The two outer columns experienced a lower pin power, with the lowest value reached in column I, where the average value was only 86 % of that in column III (see table 1) .

With this power situation in mind and the postulation that cyclic operation becomes more effective for FCMI as the rod power becomes higher (because pellet cracking and heeling processes become enhanced), it can be explained why we observe the highest diameter increases both in the pin section with the largest gap as well as with the smallest gap from fuel to cladding:

At the lower end of column II, we measured the largest diameter increase. This was close to the maximum power position. Cracking of the pellets upon rise to power allowed for the fuel segments to be pushed towards the cladding. Since the gap was wide it was probably not closed upon the first rise to full power and,certainly, the pellet fragments were not pushed uniformly into the open space of the gap (since there is always a hotter and a cooler side around a fuel pellet). Crack healing by evaporation/condensation processes produced an ovalized pellet form which was capable of straining the cladding during the following power cycles. In fuel column III, the power was practically the same, the gap, however, was smaller. There was not so much space to deform the pellet and, in addition, there was not as much expanding material in the centre of the pellet to push the fuel segments against the cladding. The stack consisted here of

hollow pellets. This is why there is also less ovality of the cladding in this pin section. The outer fuel columns which experienced less power and attained, consequently, less burn-up, caused very different diameter increases. Column IV, the lowest in the fuel pin, showed practically the same diameter increase as fuel column II, where the maximum was measured. The reason for the relatively high cladding strain is certainly the small gap of 121 µm diametral, which allowed for an early fuel cladding contact by normal fuel swelling. Column I, the upper most fuel stack, experienced the lowest rod power and the lowest degree of burn-up. The gap with 185 µm diametral was relatively large. So it is only logical that the lowest cladding deformation was measured here.

With the post-test measurements at hand one was able to disclose the error behind the erratic diameter readings of the in-pile measurements. As Fig. 4 shows, there was no diameter increase in the breeder sections inbetween the fuel columns. The in-pile readings, however, indicated a sometimes even drastic diameter change in these sections. It became obvious that there was, during many measurements, a drift of the zero value in going from top to bottom. A re-evaluation of the charts taking the expansion of the nearest breeder section as zero expansion indicated that there was actually no diameter increase during the first 7 cycles. It did not become clear wether there was a diameter change during the next 6 or 7 cycles, but it appears as if from cycle 14 to 15 onward there was diameter increase. The last measurements taken in-pile agree fairly well with the ones taken out-pile (in the limits of plus or minus a couple of microns). Still, it is not possible to follow the diameter change from cycle to cycle even by the corrected values measured in-pile.

Gamma spectrometry

As mentioned earlier, the gamma measurements were done about 8 months after reactor shut down (exactly 238 days), which means that the short lived fission products, like Te-132 and I-131, had disappeared. The interesting isotopes left for investigation were the two cesium isotopes Cs-137 and 134, as well as Ru-106 and Zr-95. Ru-103 could also be detected; after a cooling time of 6 times its half life, there was still about 1 % of the original material available. The axial gamma scans of all the above mentioned isotopes are reproduced in Figs. 6 to 10. Zirconium is the element the least likely to be moved during operation. Its gamma scan in Fig. 6 shows the position of the individual fuel stacks. Dips in the trace line in general mark pellet interfaces; large dips, like in the upper column,

indicate lower fuel density positions. Note, that there was fission product generation in the breeder pellets.

Ruthenium is generally considered as an immobile element in the fuel. The gamma scan in Fig. 7 indicates, however, axial agglomerations in practically all four fuel columns, especially in the two lower ones. Since ruthenium is a partner in metallic inclusions, the Ru-106 peaks mean agglomerations of metallic material in the columnar grain region or in the central channel. The transport of metallic fission products into the central channel has been described before /2/. Fission products forming precipitates, metallic or oxidic, get collected by migrating pores and carried along up the temperature gradient where they eventually arrive in the central channel. These agglomerations of metallic fission products occurred preferentially in fuel column III, which was made up of hollow pellets, and in the upper part of fuel column IV, the fuel stack with the smallest gap to the cladding. In column II with the large gap, the gamma scan indicates metallic agglomerations only in the lower end, where the power was the highest. At the positions with high Ru-106 intensities, ceramographic cuts were prepared and analysed. We will hear about this later.

The axial gamma profile of Ru-103 (Fig. 8) does not ressemble that of Ru-106. This fact can have two reasons. First, the specific gamma signal for Ru-103 was too weak, since only 1 % of the material available at reactor shut down was still present. A second reason could be the fuel behaviour after prolonged irradiation: The Ru-103 measured was created during the last few cycles. At this time, practically all the void volume in the gap and in the outer fuel zone was consumed. Pore migration was perhaps less effective to accumulate metallic fission products at this late irradiation state compared to previous cycles.

The two cesium scans (Fig. 9 and 10) show the typical peaks at fuel column ends. That means, this volatile element was driven axially from the hotter midpart of the column to the end pellets of each fuel stack. The axial migration stopped here. There was hardly any cesium migration into the breeder pellets separating the fuel columns. This holds for both isotopes, Cs-137 as well as Cs-134. Which is astonishing, since Cs-134 normally exhibits more axial redistribution than Cs-137 as Cs-134 has Xe-133 as precursor.

The dips in the intensities of both cesium isotopes at the pellet interfaces in the upper most fuel stack (column I) are surprising (Fig. 9 and 10). Normally, the intensities of volatile fission products show peaks at pellet interfaces. The dips in column I suggest that the pellets in this stack separated upon cooldown and the

cesium was sitting on the fuel surface and not on the cladding, or that the temperature in this pin section was very low.

Measurements on final fuel geometry

There are several means to measure the geometry of the fuel column after irradiation. One way is by painful optical investigation of betatron radiographs. It is good only if an accuracy of ± 1mm is sufficient. For fuel column lengths measurements, betatron radiography can be supported by gamma scans. For smaller dimensions, it can be confirmed by ceramography. The data gained by all three means are listed in table 2. It appears as if the betatron values for the column length are off by 1 or 2 mm. By comparing table 1 with table 2 it appears as if only the upper fuel column experienced a significant lenght increase. The central channels seem to have approximately the same length. Column I had the relatively longest and column IV the relatively shortest central hole. The relative lenghts have something to do with smear density more than with linear power. The same holds for the diameter. Column I experienced an extension of the channel due to cracking and elongation of the upper pellet. The cracks introduced new void volume which was transported into the centre, what not only extended the channel but also enlarged its diameter. This situation is seen in the ceramographic picture in Fig. 11. The diameter of the central hole is largest at the top of the column and gets smaller towards the lower part of the stack. The value given in table 2 for the cross section comes form the end pellet where the central hole tapered off. So it is not representative for the whole channel. The true value should be in the order of 1,3 mm as measured in the lower part of the longitudinal cut. To describe this situation correctly, the values for the diameters of the central hole are not only listed for those measured on cross sections but also those from longitudiual cuts. The values from longitudinal cuts are sometimes not correct. They are likely to be smaller than in reality. This was probably the case for the longiudinal cut of column II where the values appear too small. That is why they were put in parenthesis.

Both, the minimum and maximum values for the diameters of the central channels are reported to give an idea about the ovality. The largest diameter of the central hole was observed in column III which started from annular pellets. Most ovality was found in column II which initially had the largest gap. The ovality measured for the cross section of column IV is too big. It was caused by a metallic ingot that extended into the fuel (see Fig. 17).

Table 2: Post irradiation data on fuel geometry (mm)

Column	I	II	III	IV
length: betatron	65,3	66,5	64,3	67
length: γ-scan	64	64,5	62,3	66
initial	61,5	64,5	62,2	64,9
length change	2,5	0	0	1
Central channel:				
diameter cross section	1,05 / 1,08	1,55 / 1,66	1,7 / 1,75	1,32 / (1,54)
diameter longitudin.	1,3 / 2,0	(1,1 / 1,14)	1,7	-
length: betatron	60	60	57,5	58
full pellet:				
top end: betatron	2,3	3	3,3	3,3
top end: ceramogr.	2,4	-	-	-
lower end: betatron	3,5	3,5	3,5	5,7
lower end: ceramogr.	-	3,5	3,3	-

values in parentheses: not representative

"Full pellet" in table 2 denotes the end parts of each fuel column that have no central hole. In this experiment with small fuel columns these end parts were less than half a pellet length. It is worthwile to note that "full pellets" also existed in column III. The hollow end pellets got closed by fuel condensation. This was seen in the betatron radiographs and later confirmed by ceramography. In this experiment, there was no difference between the "end plugs" of a hollow and a full pellet stack.

Ceramography

Altogether eight ceramographic mounts were prepared, five cross sectional and three longitudual cuts. Their repartition is shown in Fig. 1. Micrographs of these sections together with the respective alpha- and beta-autoradiographies are

shown in Figs. 11 through 17. The goal of the ceramograpic investigation was fuel and fission product behaviour and fuel/clad chemical interactions (FCCI).

Fuel and fission product behaviour can be studied with the help of the autoradiographic images and by electron probe analysis.

Any structuring in alfa autorodiographs is due to changes in plutonium concentration. In beta autoradiographs any intensity increases or pecularities within the fuel and in the central channel are due to ruthenium concentration. Intensities in the gap and the outer fuel rim are caused by cesium isotopes. Such characteristics are found in all the images reproduced in Figs. 11 through 17. The alfa pictures show plutonium enrichments around and along the central channel with a corresponding depletion inside the columnar grains region. In the beta pictures, there are high intensities within the columnar grains region, sometimes accumulated directly along the border line of this region, as in Fig. 12, but mostly around or near the central channel. The high beta intensity is due to Ru-106 decay. It signals the presence and the positions of metallic inclusions. The intensities in the radial cracks extending to the outer fuel rim are also due to Ru-106. The illumination of the gap and the bright spots at the end of the radial cracks are due to the presence of cesium. What both types of radiographs show is that the mechanism forming the columnar grains, namely pore migration, is also responsible for the plutonium transportation to the centre and the radial redistribution of the fission products. Pore migration is the result of a vaporization condensation process caused by the temperature difference across the radial extension of the pore. In a pore, less volatile material is separated from more volatile material. The latter is preferentially evaporated at the hot side of the pore (ceiling) and condensed on the cooler side (bottom). The less volatile material stays on the ceiling and is driven up the temperature gradient as the pore moves along.

The pore scavenges all the material in its way. Gaseous fission products find an easy escape route down the temperature gradient by the tubular channels along the columnar grains created by the pore. Non-soluble fission products, metallic or ceramic, accumulate in the pore, form inclusions and are dragged further to the centre by every passing pore. Eventually, they arrive in the central channel. The results of this process can be seen in Figs. 16 and 17. In Fig. 16 we observe metallic and ceramic fission products accumulated in the lower part of the central channel. Both types of fission products must have been liquid when they arrived at their final position. The ceramic material is a eutectic between $BaUO_3$ and the

fuel. It is actually three phase as was shown in a microprobe analysis of a similar experiment /3/: the three phases are: $BaUO_3$-type with molybdenium, technetium, zirconium and plutonium additions, $(U,Pu)O_2$-fuel, and BaO. The eutectic melting temperature between $BaUO_3$ and UO_2 is tentatively given as 2100 °C /4/. This means, we should be prepared to have molten fuel containing phases in the central channel at about 2000 °C for higher burn-up pins. That this eutectic actually contains plutonium can also be detected in the respective alfa autoradiographies.

In Fig. 16 we notice that the end part of the inner hole of the annular pellet stack is closed. This was obviously achieved by fuel condensation. According to the alfa picture, there is no difference in plutonium concentration between the original pellet and the condensate in the former hole as one would expect from the different vaporization behaviour of plutonium and uranium oxide. There is indeed no inhomogeneity what so ever between the condensate and the original pellet region, not even in structure . Even the increase in plutonium concentration around the central channel is not interrupted. The closure of the hole must have happened during the early stage of operation. This would explain why there was no uranium/plutonium separation in filling the hole. The initial O/M-ratio was low (see table I). At a low O/M ratio, the fuel vapour contains as much plutonium as the solid phase. At one time or another, however, the separation mechanism worked or else the plutonium concentration would not have increased around the central channel.

Another particularity observed by ceramography was the elongation of the upper pellet of the upper fuel column. The rod power at this position was the lowest, the diameter of the central channel, however, the largest (see table 2). The elongation of the fuel obviously created new void volume in the outer fuel region which was transported (by pore migration) to the centre. From Fig. 11 it is obvious that the elongation was brought about by the unrestrained thermal expansion of the hot central region of the pellet. The upper pellet experienced an elongation of something between 1.2 and 1.4 mm, that is about half of what the whole stack achieved. This expansion created the cracks that opened up on the periphery of the pellet, and thus provided for the void volume that helped enlarge the central channel. The wide central channel here at the upper end of the fuel pin was certainly not caused by overheating.

Transfer of void volume from the gap to the centre of the fuel brings us to the question of void volume redistribution. The experiment provided fuel types with

Table 3: Void volume redistribution

Column	I	II	III	IV
Fabrication:				
Pores %th. d.	3,2	4,8	4	5
Gap %th. d.	5,5	8,2	5,45	3,6
Inner hole %th. d.	-	-	3,5	0
total v. v.%th. d.	8,7	13	12,95	8,6
transferable v. v. %th. d.	8,7	13	9,45	8,6
PIE:				
Central channel %th. d.	3,9	5,9	6,6	4
transfered v. v. %th. d.	3,9	5,9	3,1	4
not transfered v. v. %th. d.	4,8	7,1	6,35	4,6
transfered / transferable %	44,8	45,4	32,7	46,5
Central chan. / total v. v. %	44,8	45,4	51	46,5

v. v.: void volume, th. d.: theoretical density

little and much void volume, repartitioned in the pores, in the gap and, in one case, also in a prefabricated inner hole. Table 3 gives the respective numbers for each fuel column and also for the volume of the central channel formed during irradiation. A distinction is made between available void volume and transferable void volume because in the case of annular pellets all of the available volume is not transferable (the part in the inner hole).

The volume of the final central channel was calculated from the ceramographically determined diameter that was believed to be applicable for the respective column. From the table we see that only about half of the void volume from pores and the gap is transfered to the central channel in case of full pellets. For annular pellets this percentage is even smaller. In both cases, however, the central channel assembles about 50 % of the initial void volume.

It has already been stated that the so called solid fission products are carried up the temperature gradient into the centre of the fuel by migrating pores. More

pore migration should lead to more fission product transport and hence more accumulation in or around the central channel. More pore migration should be brought about by more void volume that is transferable. In other words, large fuel-to-cladding gaps should bring about more solid fission product accumulations in the centre of the fuel than small gaps. In this experiment, the contrary was the case. The fuel column with the smallest gap (col. IV) and the fuel column with the least amount of void volume tranfered (the annular pellet stack, col. III) exhibited the highest degree of solid fission product accumulation in the centre. This was already demonstrated by the gamma scans (Fig. 7) and could be confirmed by ceramography. The column with the largest gap (col. II), on the other hand, showed relatively little accumulation in the centre. Even though void transfer actually occurred, otherwise we would not have gotten the large central hole. This means, that not just any pore migration is also capable of transporting metallic or ceramic inclusions. What we notice in column II is accumulation of solid fission products along the base line of the columnar grains region. Accumulation took place where the migrating pores started from, but obviously got stuck by some reason or other.

It appears hard to find a physically meaningfull and consistent explanation for this kind of behaviour. One could evoke a smaller temperature gradient in a fuel with a large gap, since the temperature gradient is the driving force of the pore migration process. A smaller temperature gradient can appear if the fuel temperature at the base line of the columnar grains region is about or higher than 2000 K. For the same heat flux the temperature gradient would be smaller by about 5 % if the temperature in the large gap pin was higher by about 200 K than in the small gap pin, according to calculations done with thermal conductivity values given by Philipponeau /5/. However, wether such a small variation in temperature gradient could make the difference in transport capability of the process remains questionable.

MIGAS and microprobe analysis

Sample 5 of fuel column IV (see Fig. 17) was subjected to micro gamma scanning and to microprobe analysis. The main interest focused on the metallic ingot in the central channel. From a first glance it appears as if this ingot was composed of two phases (Fig. 18). The annalysis with the MIGAS system (MIcro GAmma Scanner) revealed a relatively high Sb-125 activity in the second phase, whereas the main phase was high in Ru-106. The microprobe analysis than showed that it actually consisted of three phases. The main phase, which made up the major part

of the metallic ingot, was rich in ruthenium and molybdenum. The other two phases observed on the rim of the ingot were rich in palladium and contained significant amounts of iron. The exact compositon of these phases is given in table 4. The needles, which can be seen in the multiphase region of the ingot in Fig. 18, have the same composition as the main phase. According to /6/ the main phase is the well known ε-phase containing Mo, Tc, Ru,- Rh and Pd usually found in burnt breeder reactor fuels. The rim phase 2 which contains in addition to Pd and Fe also Mo, is a Pd-Mo-Sn-Fe solid solution, and rim phase 3, which contains no Mo nor Ru, is an intermetallic phase of the composition (Fe, Sn)Pd_2. In Fig. 18, rim phase 2 appears as grains and rim phase 3 as a grain boundary phase in the multiphase region on the rim of the ingot.

Table 4: Composition of the metallic ingot in the central channel of column IV, sample 5. (values are given in at %) /6/.

Element	main phase	rim phase 2	rim phase 3
Fe	6	10	19
Mo	34	16	0
Tc	7	1	0
Ru	26	5	0
Rh	8	4	0,5
Pd	19	43	67,5
Sn	0	15	9
Sb	0	5	2
Te	0	1	1

A detailed describtion of the microprobe analysis is given in /6/. It showed that the radial Pu-concentration behaved as revealed by the alfa-autoradiography: There was a visible Pu-increase from about 0,5 r towards the central hole. The maximum concentration was 18 % PuO_2 near the central channel; the average over the cross section was 13.2 %. Zr and Nd did not show the same behaviour.

Their concentration profiles remained flat. In an earlier KAKADU experiment /7/ a similar profile as that of Pu was observed for these two elements. Traces of Cs and Xe could be found all over the cross section, with Cs in the 1 to 2 % range, and Xe with about 0.1 to 0,2 %.

The average Pu-concentration of 13.2 % in sample Nr. 5 leads to the calculation of a burn-up of about 8 %. In a fuel with an original encrichment of 21.2 % and a burn-up of around 10 %, the transformation of Pu-isotopes to elements of higher proton number matches that of the generation of plutonium from U-238 /8/. Hence, the difference between the initial and final Pu-content gives the burn-up value for this experiment.

Fuel Clad Chemical Interactions (FCCI)

Inner corrosion, another word for FCCI, took place in all four fuel stacks. The penetration depth or cladding wastage was the highest along the two inner fuel columns where the maximum observed reached 40 µm. It was much less in the outer columns, with a maximum of 20 µm in the upper and of 25 µm in the lower fuel column (see also table 5). The type of cladding attack was clearly a uniform matrix attack without any preceding attacked grain boundary zone. The reaction zone was formed of metallic and oxide reaction products ("mottled zone"). The metallic phase was concentrated on and near the fuel surface. Penetration of metallic products into the fuel occurred both along grain boundaries and pellets cracks. These latter penetrations are known as "iron rivers" since they consist almost entirely of iron. The iron is one of the reaction products with the cladding. It results form the complex chemical reaction:

$$Cs_2Te + \left[O_2 \right]_{fuel} + \left[Fe, Cr \right]_{clad.} \Rightarrow Cs_xCrO_4 + Fe\,Te$$

The condensed fission products Cs and Te attack in a synergistic effort the cladding. Cs forms, mainly with Cr, the oxidic reaction products and Te, mainly with iron, the reaction products that become later metallic. The tellurides are intermediate reaction products. They decompose near the hot fuel surface and leave behind a metallic phase which is basically iron with some nickel and rarely, for low oxygen potentials only, little chromium.

The chromium tellurides that form in the primary reactions are normally further transformed into oxides. The metallic phase can move into the fuel along cracks and grain boundaries. As soon as it reaches the columnar grain region it can be

Table 5: Inner corrosion results (Penetration depths and width of reaction zones)

Column Nr.	Sample Nr.	Max. pen. depth µm	React.zone µm
I	7	0	
	1	20	20
II	2	40	85 (140) *
	8	40	50
III	3	40	130
	4	10	30
IV	5	25	70

* one location

dragged along by migrating pores if pore migration is still in progress. In cyclic operation, this process can go on over the whole irradiation period. The fact that iron was found in significant amounts in the metallic ingot in the central channel of sample Nr. 5 proves that the pore migration process was still working after inner corrosion took place, and with a gap filled with reaction products. Table 5 lists the maximum penetration depths for the cladding attack in each of the four fuel pins. The extent of the reaction zones between fuel and the intact cladding are given as an indication of the reaction volume along each fuel stack. The cladding reactions seem to be a function of the axial position or the neutron flux (see Fig. 19). Since the neutron flux determined not only the linear power but also the inner cladding and fuel temperature, a clear distinction between the effect of power and temperature cannot be made. Also, the deepest attack occurred along the two low smear density fuel stacks with only little less overall cladding reaction in the annular pellet stack compared with the fuel column with the wide gap. It is expected that low density fuel brings about more cladding attack since fuel temperature is higher and release of aggressive volatile fission products enhanced. A similar effects should come from a wide fuel-cladding gap, which appears to be in agreement with the findings here. However, due to the attack profile observed in the individual fuel columns, it is believed that the high neutron flux and its consequences on the thermal regime was responsible for the relative higher corrosion along the inner two fuel columns.

In evaluating the cladding corrosion results of this experiment it must be remembered that: First, the fuel columns were very short. There was little, if any, axial accumulation of aggressive fission products, that means, the reactions with the cladding had to put up with the fission products made available by the local fuel cross section. Secondly, the initial O/M-ratio was low. And a burn-up of about 8 at % is not high. Hence, it is not farfetched to assume that the cyclic operation mode had something to do with the corrosion results.

Concluding remarks

The original goal of the MEDINA experiment, the determination of incremental diameter increases after power ramps, could not be achieved. The in-pile diameter mesurements were useless. Apparently, the signal processing did not work well. Inspite of these shortcomings was the experiment not useless. It furnished valuble results about fuel and fission product behaviour in a cyclic operation mode:

Mechanical interactions between fuel and cladding took place in all four fuel columns. Cladding expansion stayed small with a maximum of 0.2 %. It was only partly dependent on gap size. Infact, the largest diameter increase was measured in the pin section where the original gap was the largest. It appears as if a large gap does not ease the FCMI situation in cyclic operation. The fuel apparently quickly bridges the gap to the cladding during power ramps.

Fuel and fission product movements seem to be enhanced by cyclic operation. Large quantities of solid fission products in the central channel and large reaction zones in the gap between fuel and cladding were observed for these short fuel stacks. Both ends of the annular pellet column were closed by fuel condensation. Pore migration was activated throughout the experiment. It was even capable of transporting cladding reaction products into the central hole.

Acknowledgements

Acknowledgements go to Fa. Alkem,Hanau,for the fabrication of the unique MEDINA pin, to JRC Petten for making available the irradiation capsule and for the operational data recording and processing, to ECN Petten Hot Labs for the non-destructive P.I.E., and to the Hot Cells of KfK for the careful destructive P.I.E. work.

References

/1/ F. Mason: Description of an Experiment for the Irradiation of FBR Fuel Pins with Intermittent Diameter Gaging D170-02-POCY/02 CEC Technical Memorandum IT/84/2149.

/2/ O. Götzmann: LMFBR-fuel pin behaviour. Fast rector core and fuel structural behaviour. BNES, London, 1980, proceedings, p. 1
also: Fission product behaviour in fast breeder fuel pins, J. Nucl. Mater. 188 (1992) 58.

/3/ H. Kleykamp et al: Nachuntersuchungen am Bestrahlungsexperiment Rapsodie I, Teil II: Stab BM-06. PSB-Bericht Nr. 1192 (Phase II b) vom 12.5.1977. Internal Report

/4/ Gmelin U-Erg. Bd. C3.

/5/ Y. Philipponneau, J. Nucl. Mater. 188 (1992) 184.

/6/ H. Kleykamp; H. D. Gottschalg: Nachuntersuchungen am Betriebstransientenexperiment MEDINA-POCY02, Primärbericht 32.04.05P02B, Nov. 1992. Internal Report

/7/ H. Kleykamp, H. D. Gottschalg: Nachuntersuchungen am Betriebstransientenexperiment KAKADU II/24, Primärbericht 32.04.05 P02A, April 1992. Internal Report

/8/ H. Wiese, KORIGEN-calculations, private communication 1993.

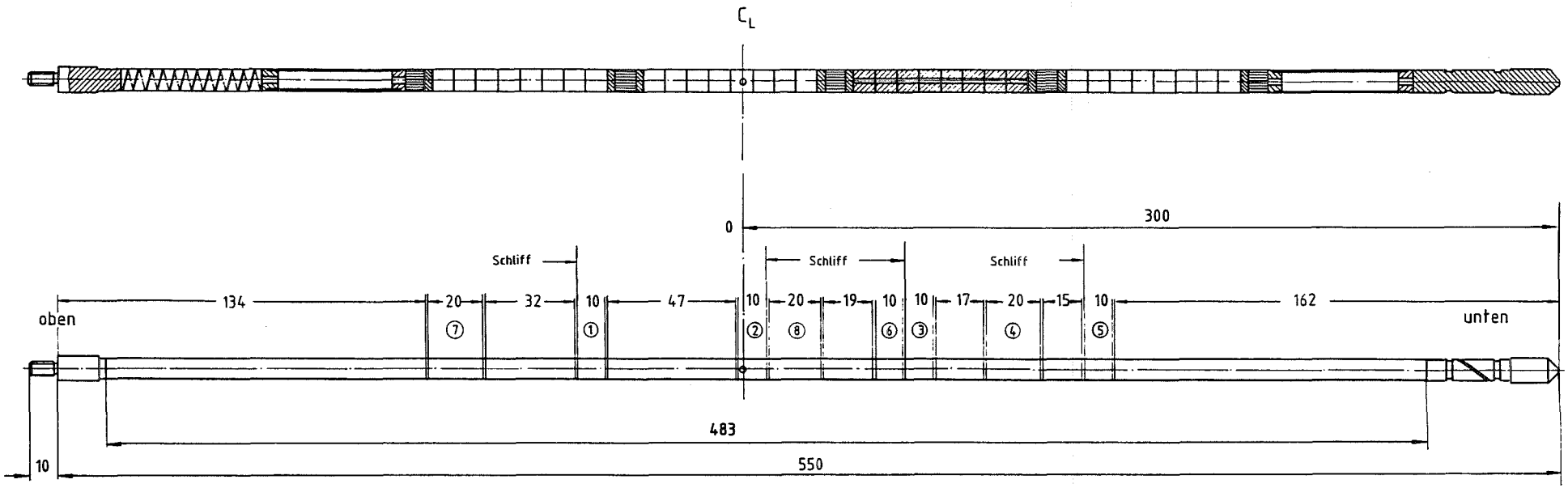

MEDINA (Pocy 02)

① KQ
② KQ
③ KQ
④ KL
⑤ KQ
⑥ Abbrandanalyse
⑦ KL
⑧ KL

(K=Keramografie)
(Q=Querschliff)
(L=Längsschliff)

Schnittbreite 1,0 mm

Fig. 1: Test pin

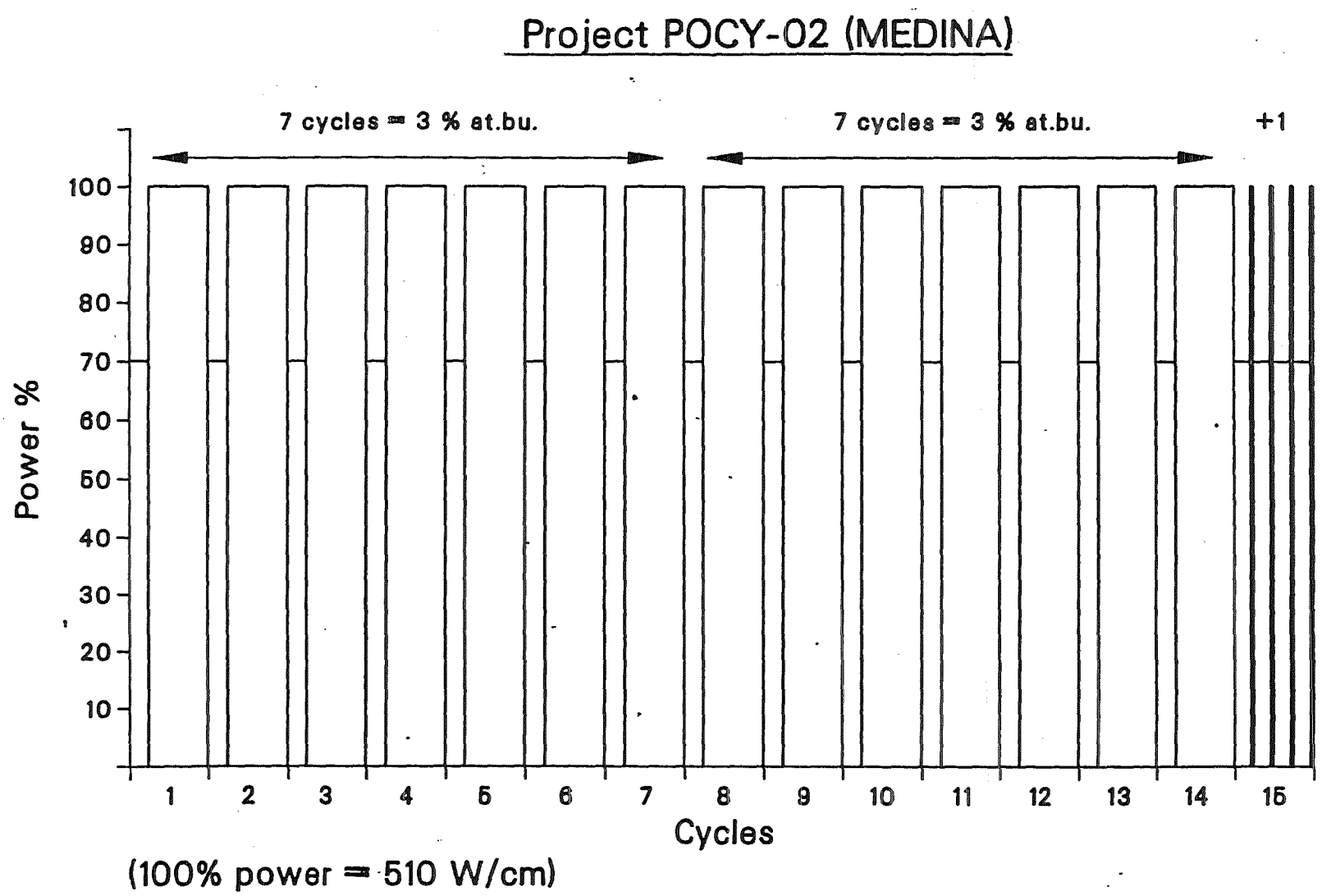

Fig.2: Planned irradiation programme

Fig. Expt. D170 POCY-02 (MEDINA)

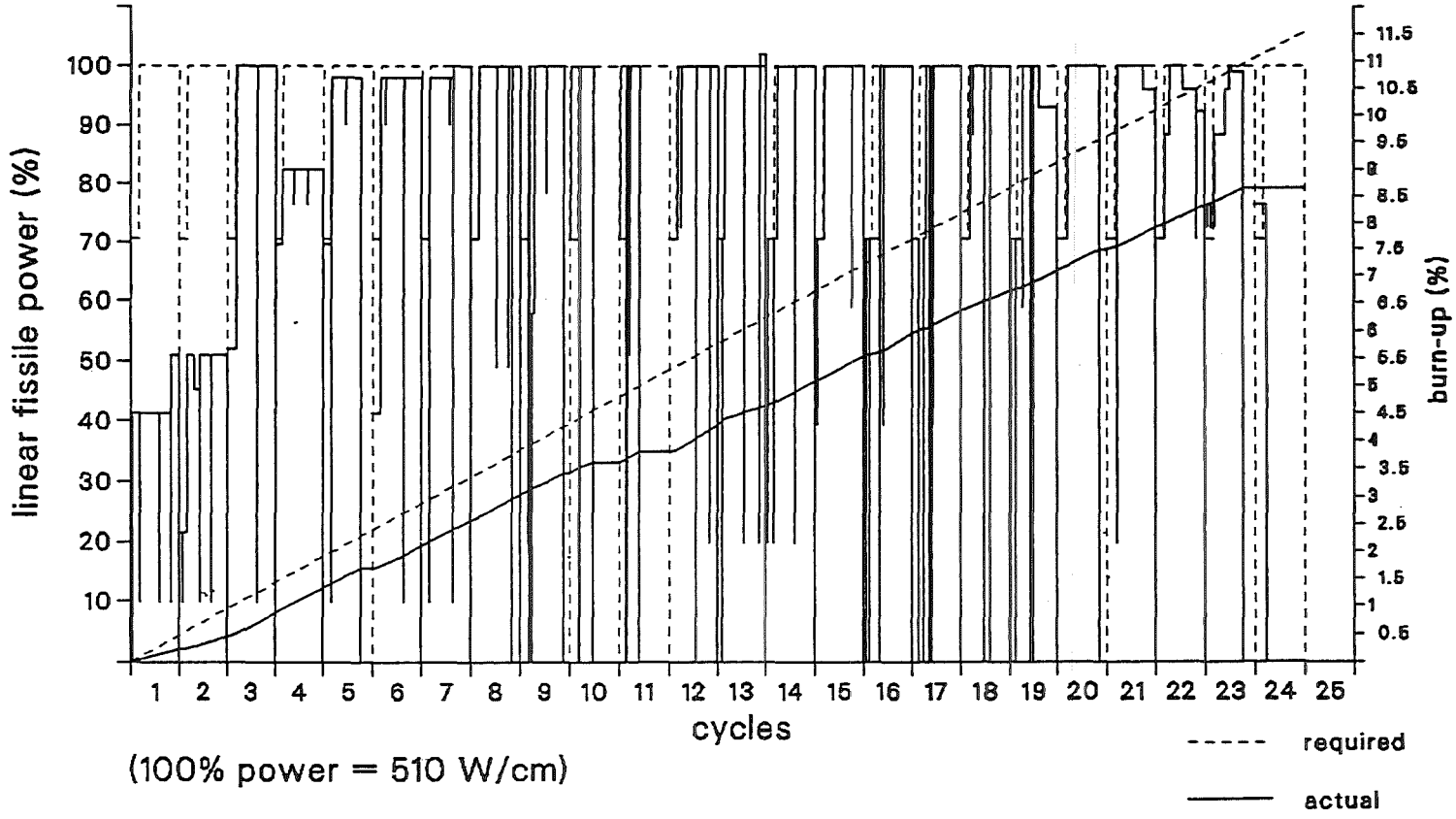

Fig. 3: Actual irradiation history

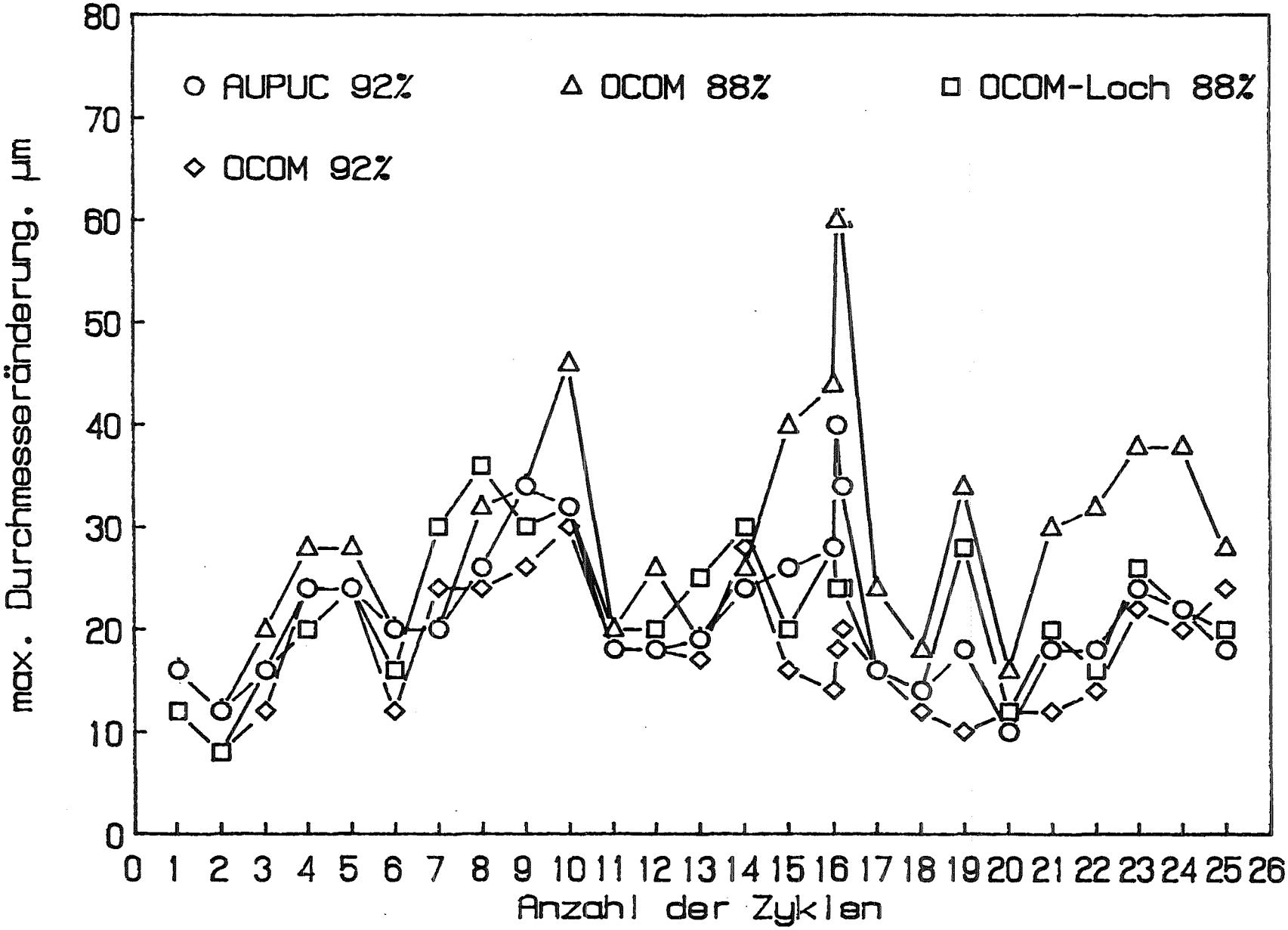

Fig. 4: Max. Diameter increase as measured in-pile after each cycle

fuel type	AUPUC	OKOM	OKOM hollow	OKOM
smear d. %	92	88	88	92
gap µm	185	275	183	121
local b. u. %	**7,26**	**8,34**	**8,44**	**7,81**

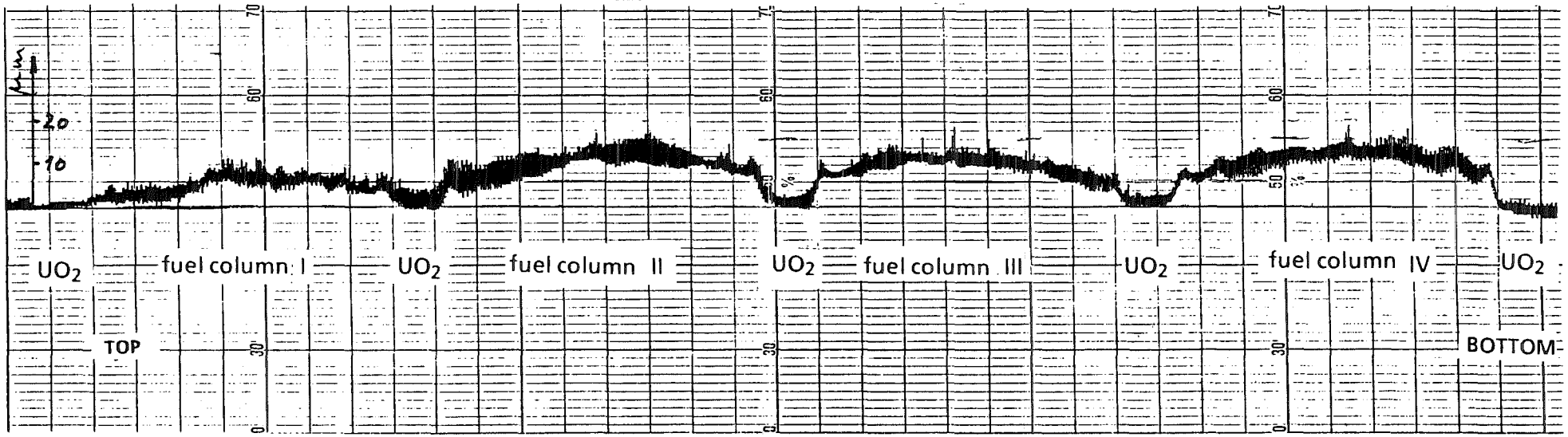

Fig. 5: Diameter profile measured out-pile

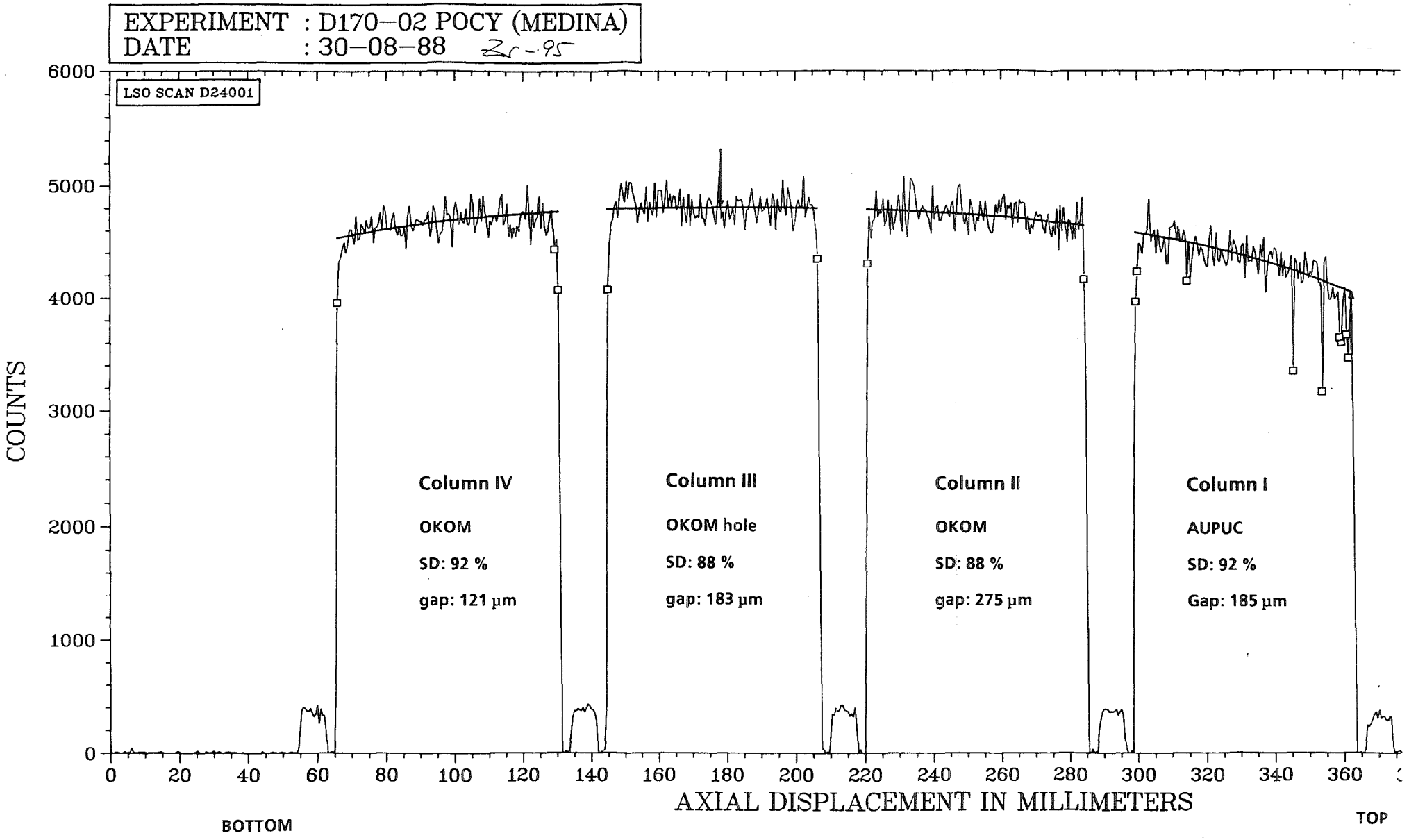

Fig. 6: Axial γ-scan for Zr-95

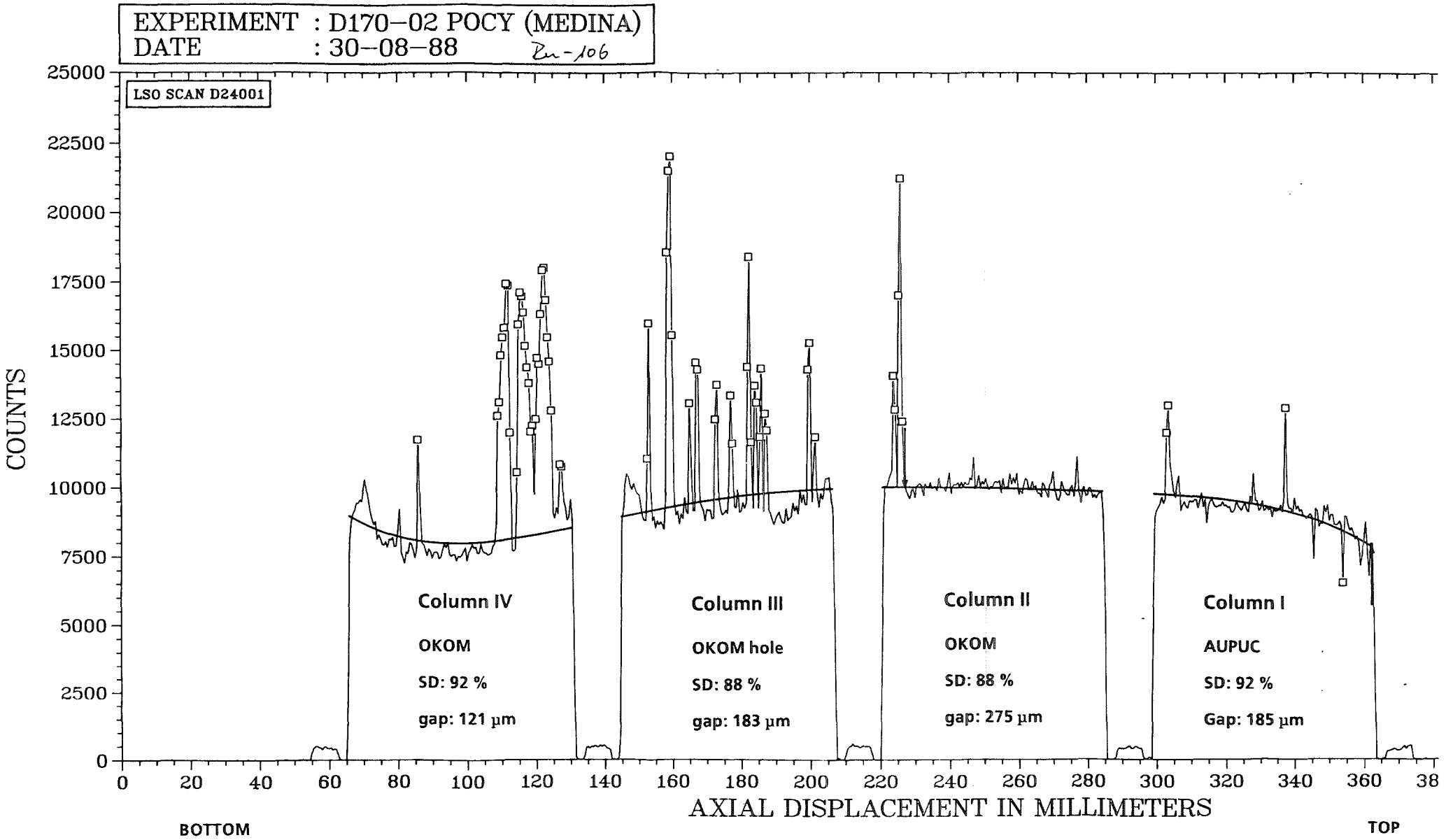

Fig. 7: Axial γ-scan for Ru-106

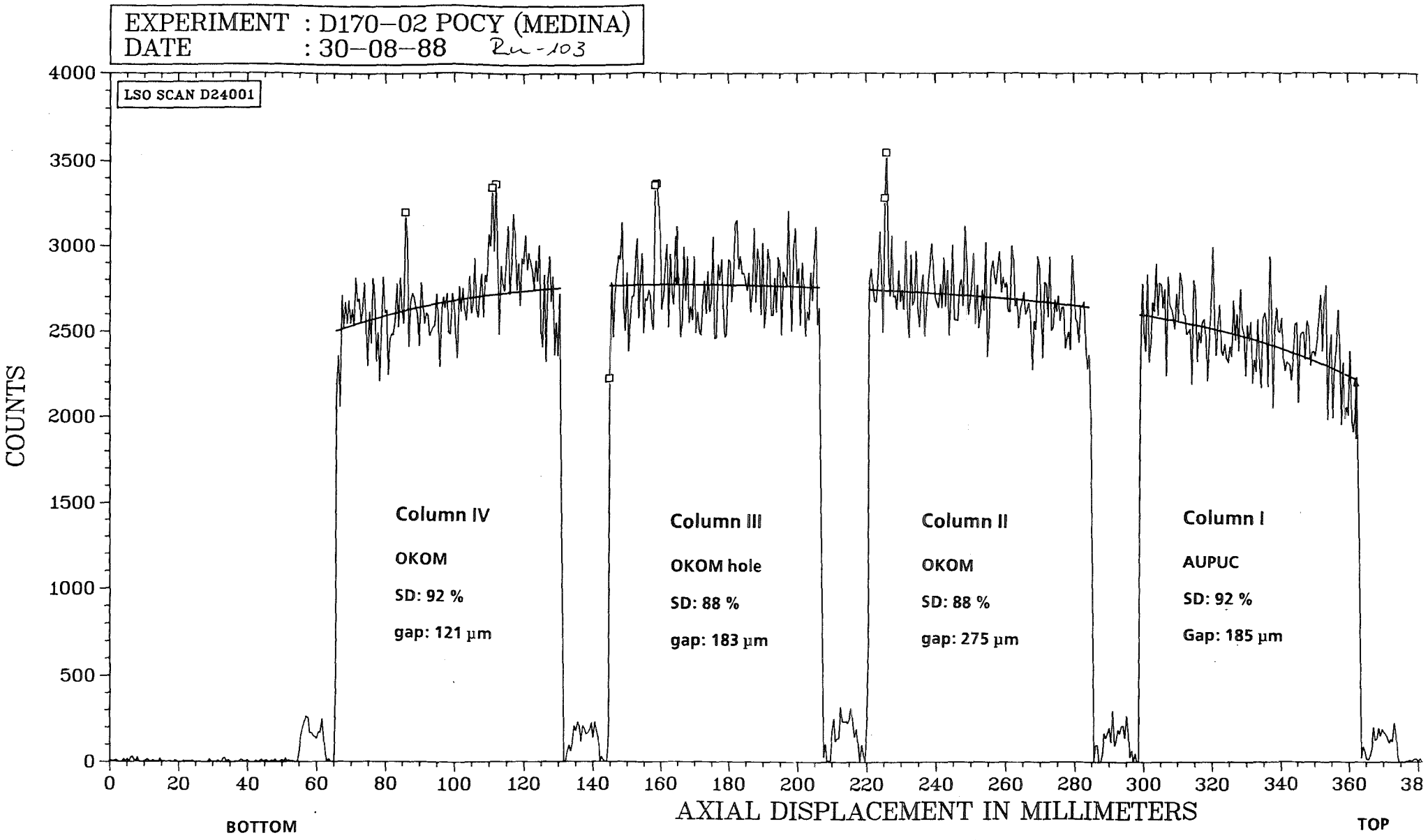

Fig. 8: Axial γ-scan for Ru-103

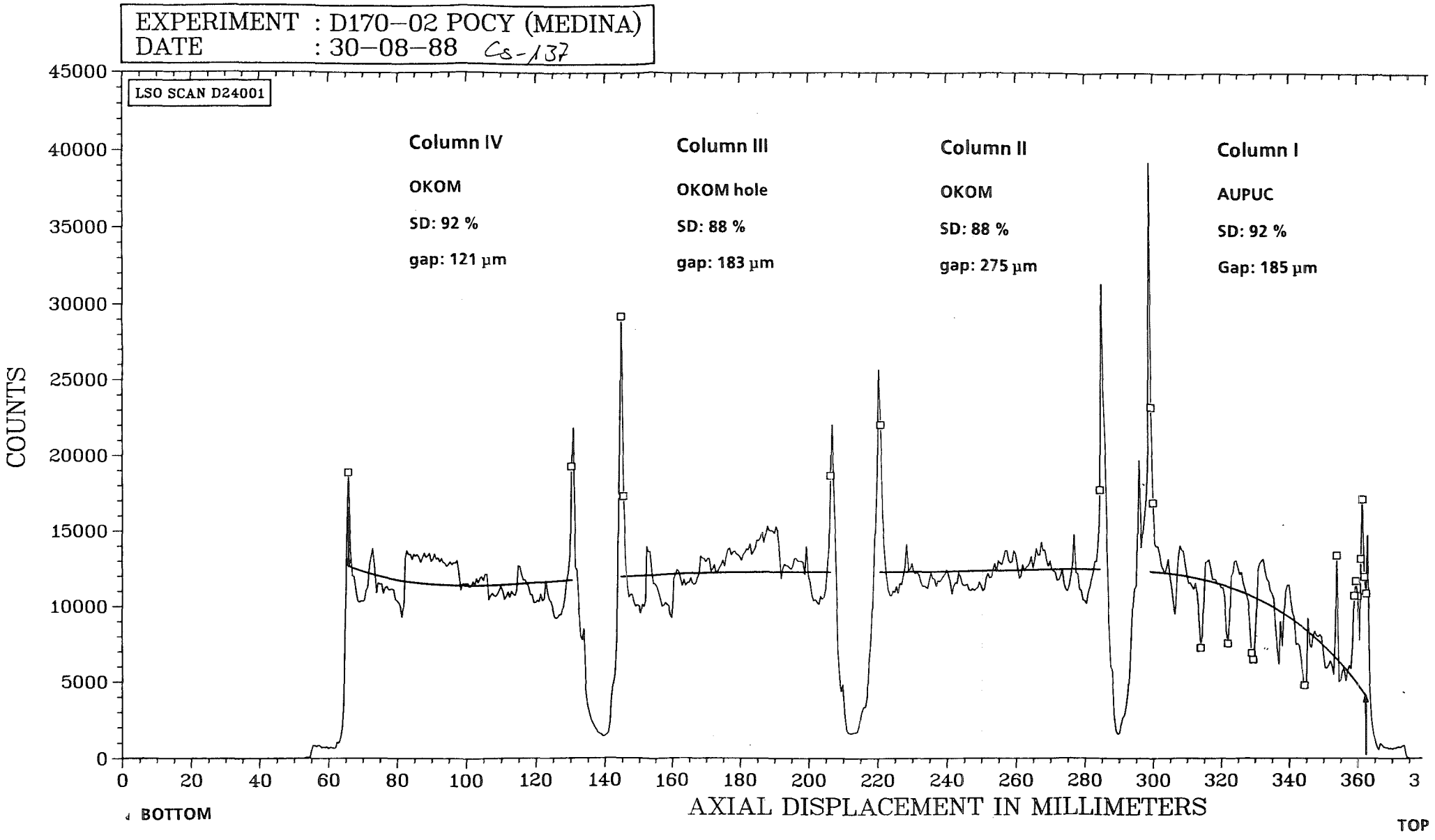

Fig. 9: Axial γ-scan for Cs-137

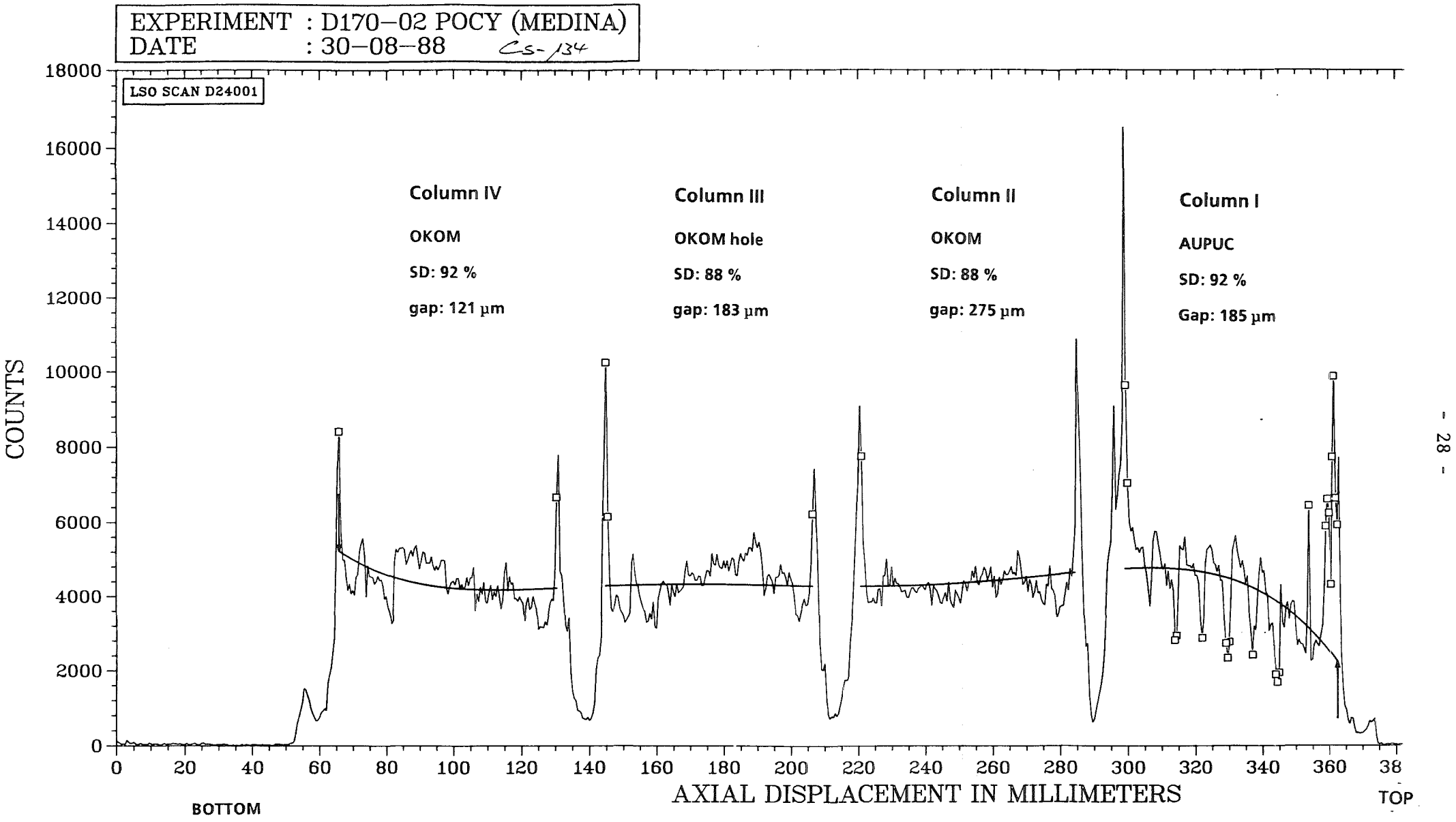

Fig.10: Axial γ-scan for Cs-134

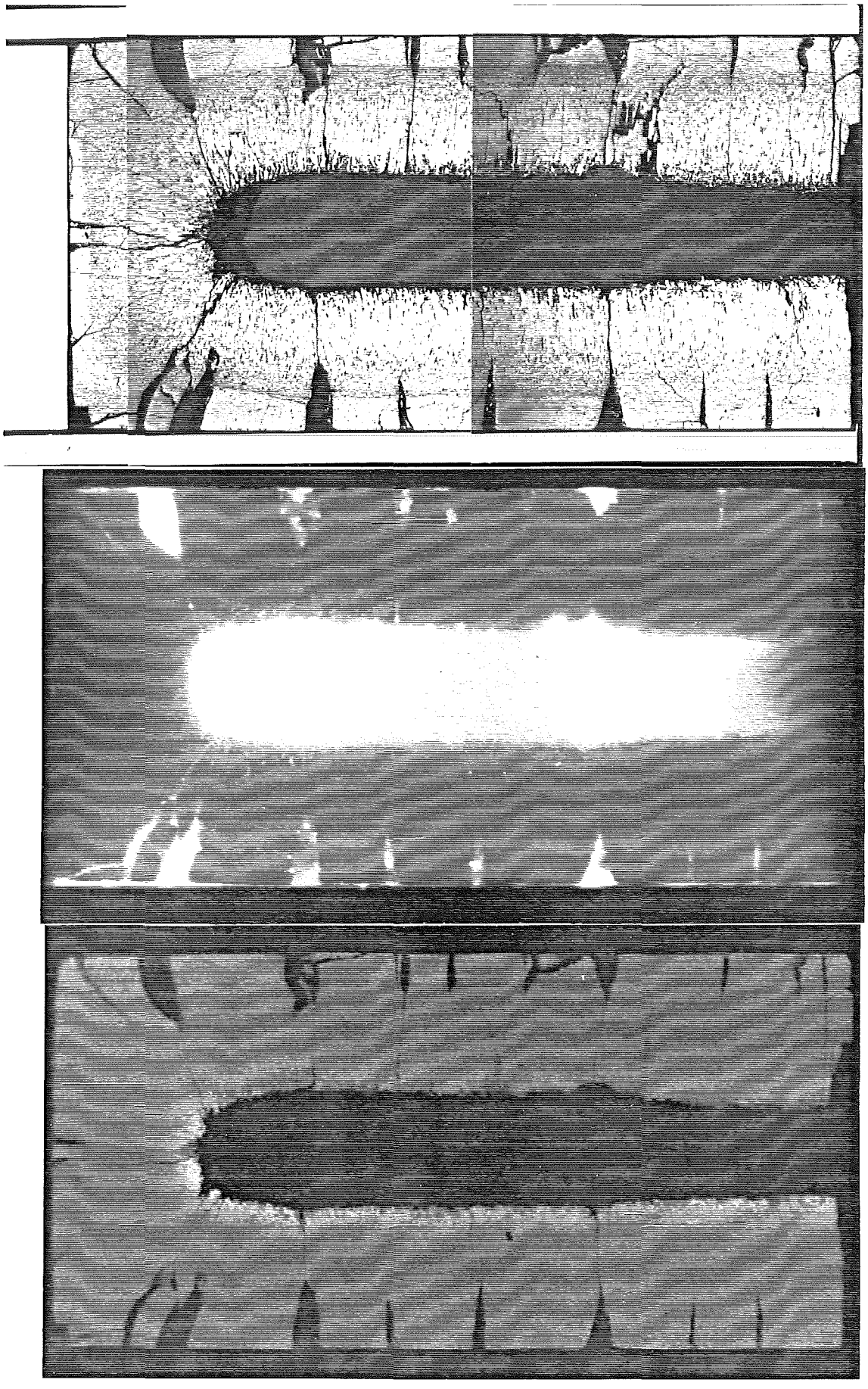

Fig.11: View of top of Column I, sample 7

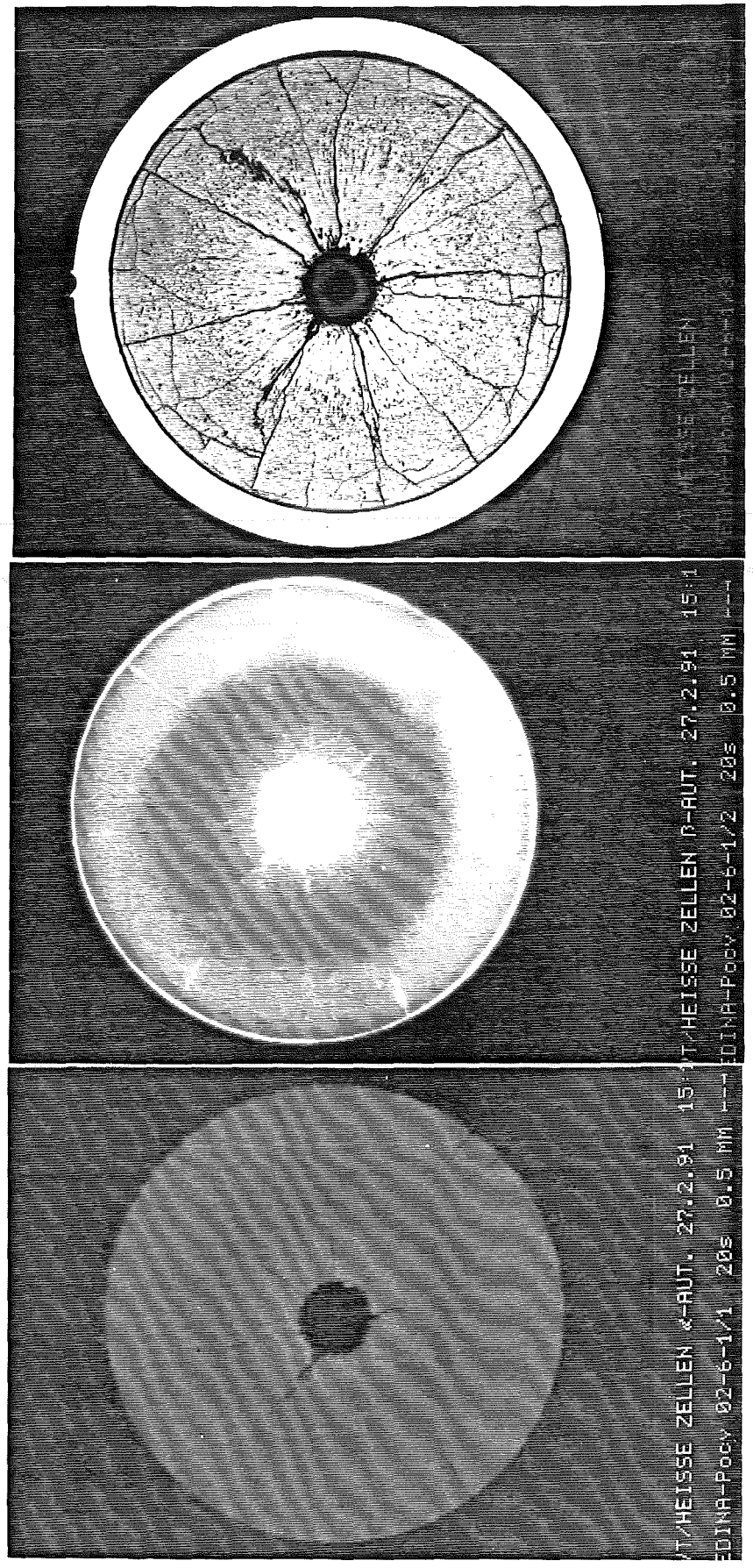

Fig.12: View of cross section at lower end of Col. I, sample 1

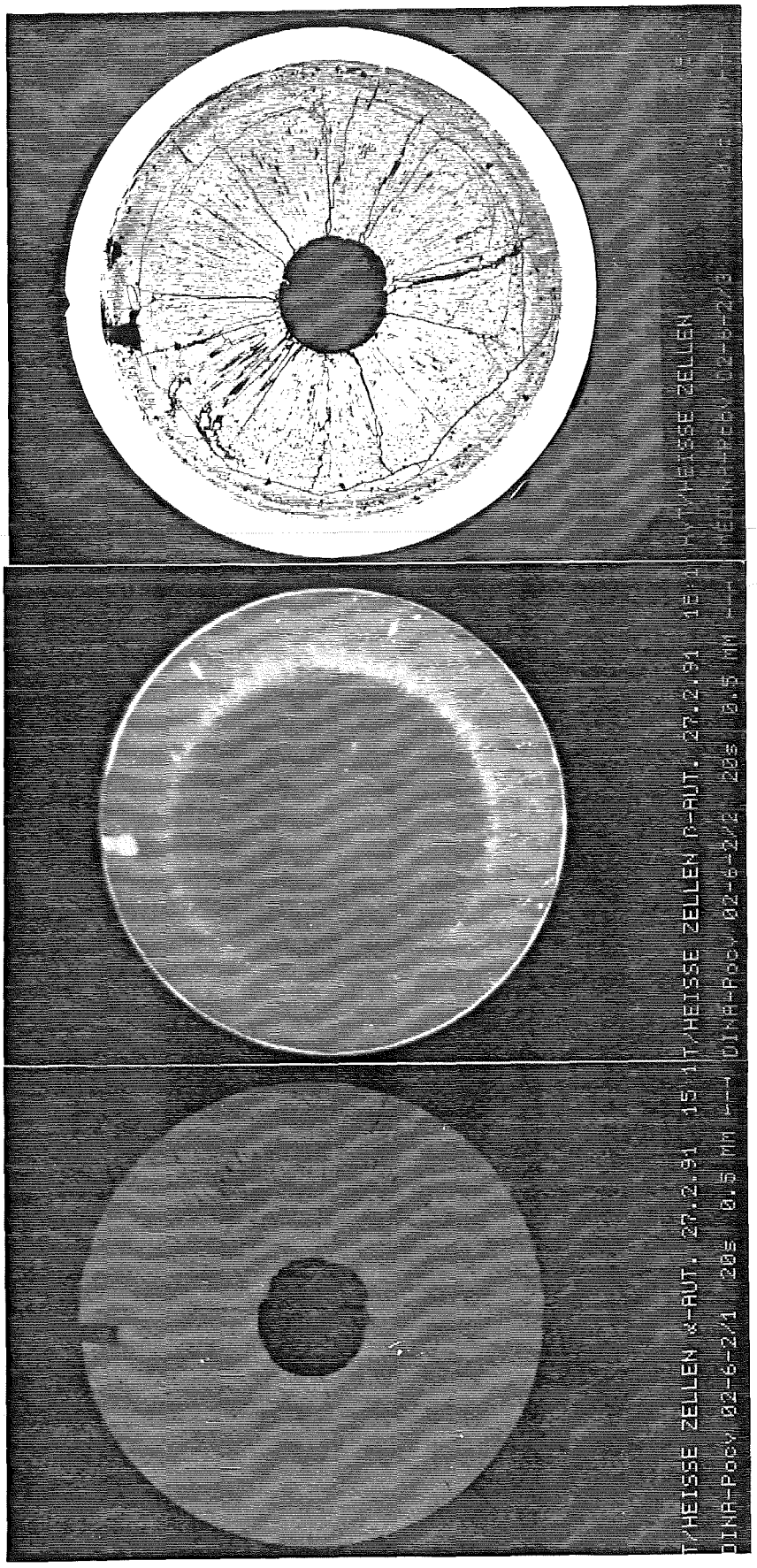

Fig.13: View of cross section at midplane of Col. II, sample 2

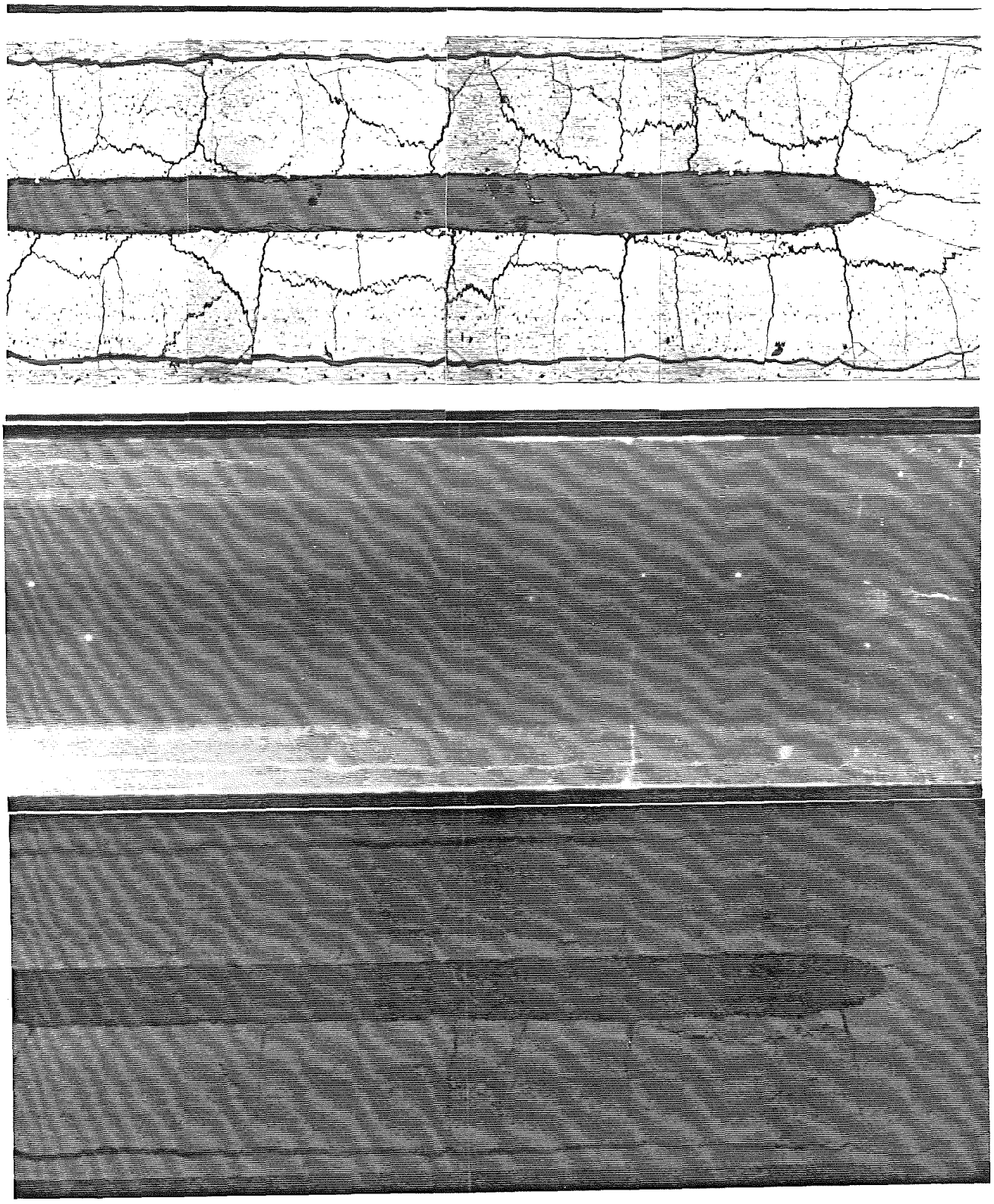

Fig.14: View of lower end of Col. II, sample 8
α-autorad; β-autorad; micrography

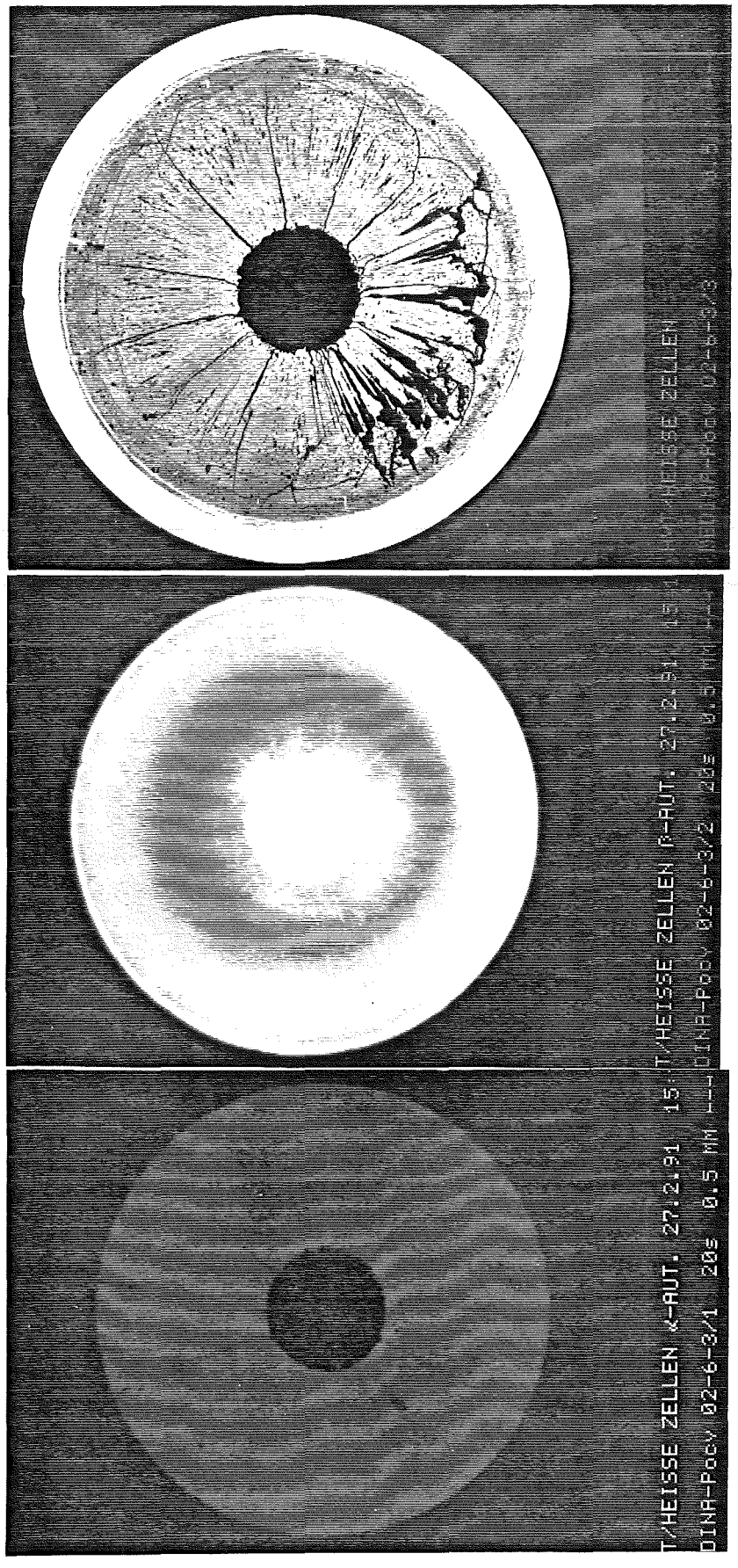

α-autoradiography β-autoradiography micrography

Fig.15: View of cross section at top of Col III, sample 3

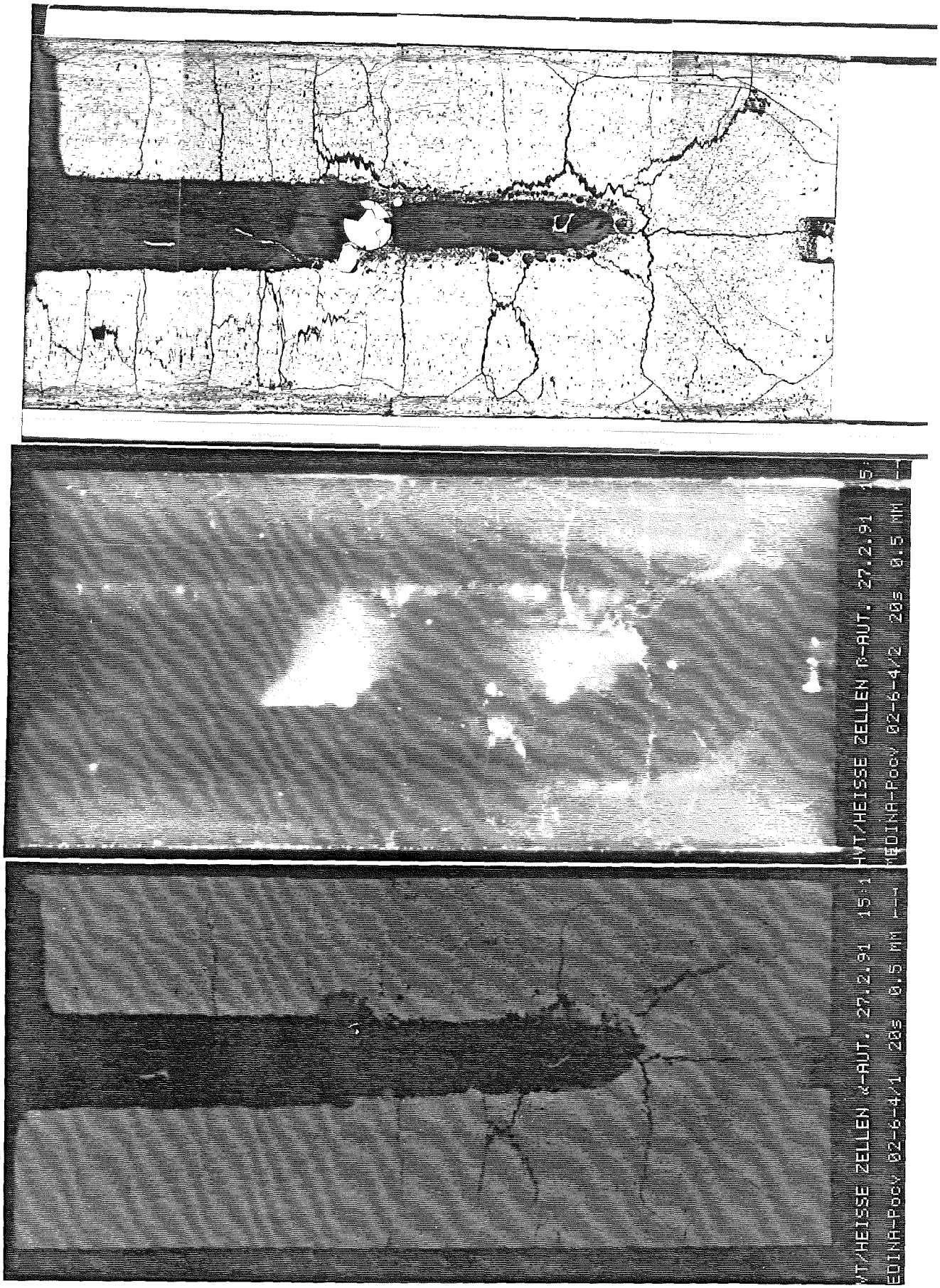

Fig.16: View of lower end of Col III, sample 4
α-autorad; β-autorad; micrography

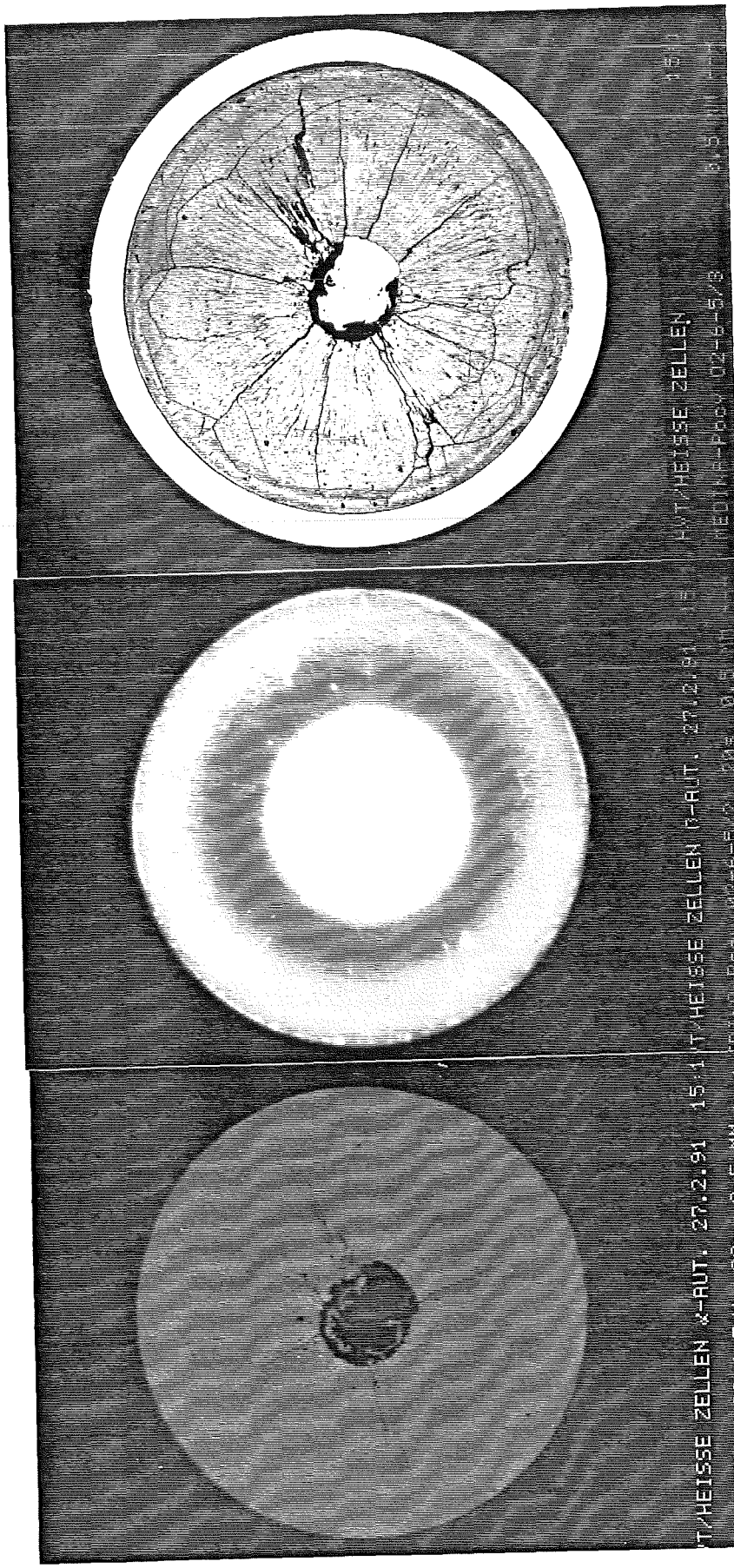

α-autoradiography β-autoradiography micrography

Fig.17: View of cross section at top of Col IV, sample 5

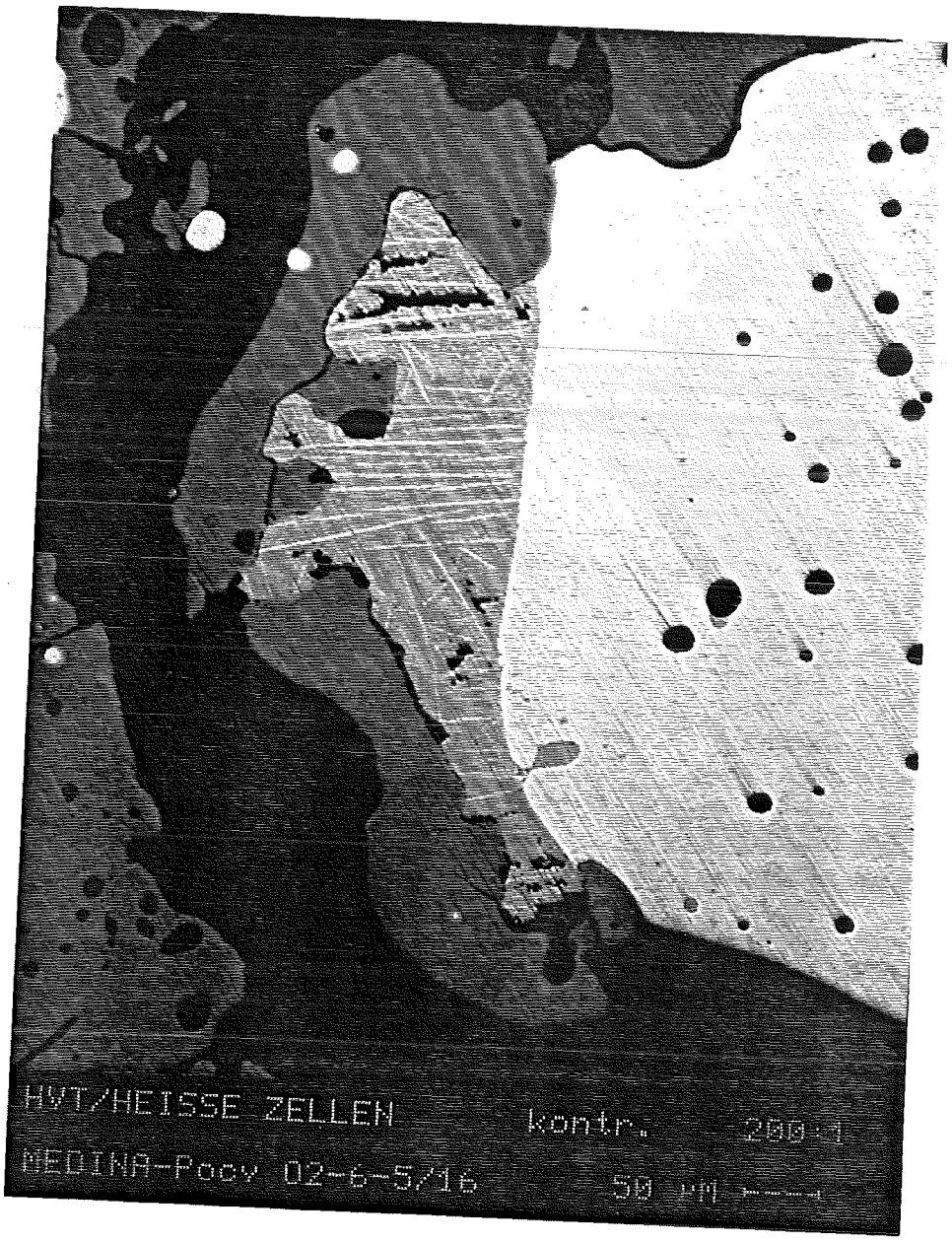

Fig.18: Detail of Fig. 17. Multiphase region on the rim of metallic ingot in central channel

Fig.19 Axial Flux Distribution in PSF 5, plus relative positions of fuel pin and thermocouples

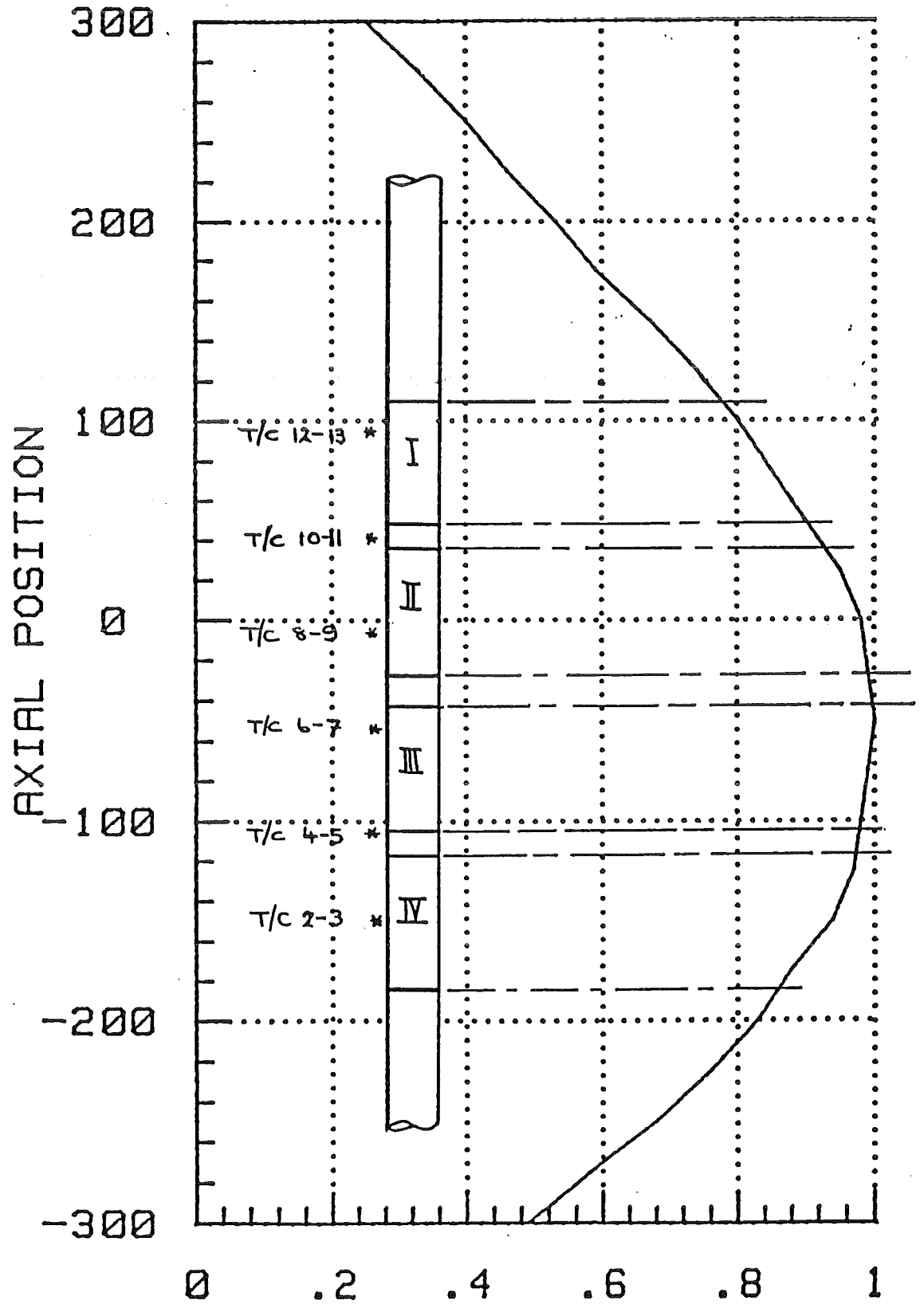

Fig.19: FLUX DISTRIBUTION